# Stabilization of a spatially uniform steady state in two systems exhibiting Turing patterns

# Stabilization of a spatially uniform steady state in two systems exhibiting Turing patterns

Keiji Konishi* and Naoyuki Hara
*Department of Electrical and Information Systems, Osaka Prefecture University, 1-1 Gakuen-cho, Naka-ku, Sakai, Osaka 599-8531, Japan*

(Received 9 July 2017; revised manuscript received 21 November 2017; published 1 May 2018)

This paper deals with the stabilization of a spatially uniform steady state in two coupled one-dimensional reaction-diffusion systems with Turing instability. This stabilization corresponds to amplitude death that occurs in a coupled system with Turing instability. Stability analysis of the steady state shows that stabilization does not occur if the two reaction-diffusion systems are identical. We derive a sufficient condition for the steady state to be stable for any length of system and any boundary conditions. Our analytical results are supported with numerical examples.

DOI: 10.1103/PhysRevE.97.052201

## I. INTRODUCTION

Over the last quarter-century, much effort has been invested into understanding the coupling-induced quenching of self-oscillations. Amplitude death, a quenching phenomenon, has been widely studied by the nonlinear science community [1,2]. This phenomenon is a stabilization of unstable equilibrium points embedded within individual oscillators through a diffusive coupling . It is well recognized that both of the following two conditions are necessary for amplitude death to occur. The first is a strong coupling strength. The second is that one or more of the following is satisfied:[1] (i) the frequencies of the oscillations differ [3–8], (ii) the diffusive connection includes a time delay [9–15], or (iii) the diffusive connection has its own dynamics [16–20].

In addition to amplitude death, the nonlinear science community has also paid considerable attention to spatiotemporal phenomena in reaction-diffusion systems [21–23]. Not only a *single* reaction-diffusion system but also a *pair* of coupled reaction-diffusion systems can exhibit interesting spatiotemporal behavior [24]. Many studies on coupled reaction-diffusion systems [25–27] have dealt with the well-known complex Ginzburg-Landau systems [28–30], in which the reaction terms are oscillatory. Our previous study [31] reported that a spatially uniform steady state in coupled complex Ginzburg-Landau systems can be stabilized under condition (i) or (ii) mentioned above.

It is widely known that, in reaction-diffusion systems, the diffusion term can destabilize the stable reaction dynamics. This phenomenon is referred to as Turing instability, which induces well-known Turing patterns [21,22]. This instability has been recognized as a fundamental mechanism for pattern generation in nature [32]. Although a variety of spatiotemporal behaviors in coupled reaction-diffusion systems with Turing instability have been investigated analytically and experimentally [33–40], to the best of our knowledge, there have been few studies on the stabilization of a spatially uniform steady state in a coupled system with Turing instability (see Sec. V for details).

The present paper investigates the stability of a spatially uniform steady state in a pair of reaction-diffusion systems with Turing instability. We focus on the simplest diffusive type of connection, which satisfies neither condition (ii) nor (iii). In addition, condition (i) cannot be satisfied for reaction-diffusion systems with Turing instability, since these systems are not oscillatory due to the stable reaction dynamics.[2] Hence, in the present paper, instead of condition (i), we assume that each system has different diffusion coefficients. These different coefficients induce different wave patterns in systems. We analyze the stability of the spatially uniform steady state in the coupled systems with different-wave Turing instability. The analytical results for the stability are verified with numerical simulations.

## II. DESIGN OF DIFFUSION COEFFICIENT RATIO

This section will review a condition for the existence of Turing instability and will present a method to determine a diffusion coefficient ratio that induces Turing instability.

Let us consider a one-dimensional reaction-diffusion system,

$$\begin{aligned}\frac{\partial u}{\partial t} &= f(u,v) + \delta\frac{\partial^2 u}{\partial x^2}\\ \frac{\partial v}{\partial t} &= g(u,v) + \frac{\partial^2 v}{\partial x^2},\end{aligned} \tag{1}$$

where $u := u(t,x) \in \mathbb{R}$ and $v := v(t,x) \in \mathbb{R}$ are state variables at position $x \in [0,L]$ and time $t \geqslant 0$. Here, $L > 0$ is the length of $x$. The nonlinear functions, $f(u,v) : \mathbb{R}\times\mathbb{R} \to \mathbb{R}$ and $g(u,v) : \mathbb{R}\times\mathbb{R} \to \mathbb{R}$, represent the reaction kinetics. $\delta \in (0,1)$ is the diffusion coefficient ratio [see Appendix A for more details on system (1)]. We assume that this system has a

*http://www.eis.osakafu-u.ac.jp/∼ecs

[1]Note that there are other conditions in addition to (i), (ii), and (iii).

[2]This means that the reaction terms $f$ and $g$, explained later, in reaction-diffusion systems with Turing instability have a stable equilibrium point (see Lemma 1 for more details).

 

spatially uniform steady state,

$$[u\ v]^T = [u^*\ v^*]^T, \quad \forall x \in [0,L], \tag{2}$$

where $(u^*,v^*)$ is an equilibrium point of the reaction kinetics, $f(u^*,v^*) = g(u^*,v^*) = 0$ .

Now we examine the linear stability of the steady state (2) using linearized dynamics,

$$\frac{\partial}{\partial t}\boldsymbol{\mathcal{X}} = \boldsymbol{A}\boldsymbol{\mathcal{X}} + \frac{\partial^2}{\partial x^2}\boldsymbol{D}\boldsymbol{\mathcal{X}}, \tag{3}$$

$$\boldsymbol{\mathcal{X}} := \begin{bmatrix} u-u^* \\ v-v^* \end{bmatrix}, \quad \boldsymbol{A} := \begin{bmatrix} f_u & f_v \\ g_u & g_v \end{bmatrix}, \quad \boldsymbol{D} := \begin{bmatrix} \delta & 0 \\ 0 & 1 \end{bmatrix},$$

where $\boldsymbol{A}$ denotes the Jacobian matrix of the reaction dynamics at equilibrium point $(u^*,v^*)$. The characteristic function of system (3) is written as

$$\begin{aligned} F(s,\gamma) :&= \det(s\boldsymbol{I}_2 - \boldsymbol{A} + \gamma\boldsymbol{D}) \\ &= s^2 + \{\gamma(\delta+1) - f_u - g_v\}s \\ &\quad + (\gamma\delta - f_u)(\gamma - g_v) - f_v g_u. \end{aligned} \tag{4}$$

Here, $\gamma := k^2$ is a parameter, where $k \in \mathbb{R}$ is the wave number. This parameter depends on the medium conditions, i.e., the length $L$ and the types of boundaries [21,32] . It must be noted that system (3) is stable for any $L > 0$ and any boundary condition if and only if all of the roots of $F(s,\gamma) = 0$ have negative real parts for any $\gamma \geqslant 0$.

Here we review the condition for the existence of Turing instability [32].

*Lemma 1:* Suppose that the necessary and sufficient condition for the equilibrium point $(u^*,v^*)$ of reaction terms to be stable,

$$f_u + g_v < 0, \tag{5}$$

$$f_u g_v - f_v g_u > 0, \tag{6}$$

holds. If two inequalities

$$\delta g_v + f_u > 0, \tag{7}$$

$$(\delta g_v + f_u)^2 - 4\delta(f_u g_v - f_v g_u) > 0 \tag{8}$$

are satisfied, then there exists $\gamma \geqslant 0$ such that $F(s,\gamma)$ is unstable.

If Turing instability occurs, then $f_u$ and $g_v$ always satisfy the following condition [32]:

*Corollary 1:* A necessary condition for matrix $\boldsymbol{A}$ to satisfy Lemma 1 is given by

$$f_u > 0,\ g_v < 0. \tag{9}$$

Now we provide a procedure for the design of the diffusion coefficient ratio $\delta$ such that Turing instability occurs.

*Lemma 2:* Suppose that matrix $\boldsymbol{A}$ satisfies the conditions (5), (6), and (9). If the diffusion coefficient ratio $\delta$ is selected from the range

$$\delta \in (0,\delta_-), \tag{10}$$

$$\delta_- := \frac{f_u g_v - 2f_v g_u - 2\sqrt{f_v g_u (f_v g_u - f_u g_v)}}{g_v^2}, \tag{11}$$

then there exists $\gamma \geqslant 0$ such that $F(s,\gamma)$ is unstable.

*Proof.* See Appendix B. ■

The next section considers the following situation: a pair of systems (1) with $\delta$ designed according to Lemma 2 are coupled by a diffusive connection.

## III. COUPLED REACTION-DIFFUSION SYSTEMS

We consider a pair of one-dimensional reaction-diffusion systems,

$$\begin{aligned} \Sigma_1 &: \begin{cases} \frac{\partial u_1}{\partial t} = f(u_1,v_1) + \delta\frac{\partial^2 u_1}{\partial x^2} + r_{u,1} \\ \frac{\partial v_1}{\partial t} = g(u_1,v_1) + \frac{\partial^2 v_1}{\partial x^2} + r_{v,1} \end{cases}, \\ \Sigma_2 &: \begin{cases} \frac{\partial u_2}{\partial t} = f(u_2,v_2) + \mu\delta\frac{\partial^2 u_2}{\partial x^2} + r_{u,2} \\ \frac{\partial v_2}{\partial t} = g(u_2,v_2) + \mu\frac{\partial^2 v_2}{\partial x^2} + r_{v,2} \end{cases}, \end{aligned} \tag{12}$$

where $\mu \in (0,1]$ represents the ratio of the diffusion coefficients for systems $\Sigma_2$ and $\Sigma_1$. Here, $r_{u,1}$, $r_{u,2}$, $r_{v,1}$, and $r_{v,2} \in \mathbb{R}$ are the connection signals, which shall be explained later.

The present study assumes that Turing instability has already occurred in individual systems $\Sigma_{1,2}$ without coupling. In order for this assumption to be valid, the system $\Sigma_1$ without coupling, which is equivalent to system (1), has to satisfy Lemma 2. It should be noted that the system $\Sigma_2$ without coupling, which has the additional parameter $\mu$, can be applied to Lemma 2, since the characteristic function for system $\Sigma_2$ is described by $F(s,\gamma\mu)$. This fact indicates that if there exists $\gamma \geqslant 0$ such that the characteristic function $F(s,\gamma)$ for system $\Sigma_1$ is unstable, then there also exists $\gamma' \geqslant 0$ such that $F(s,\gamma'\mu)$ is unstable. As a result, Lemma 2 is valid even for system $\Sigma_2$. Let us summarize the above-mentioned assumption as follows:

*Assumption 1:* Assume that system (1) has the length $L$ and the types of boundaries such that Turing instability occurs, that is, both systems $\Sigma_{1,2}$ without coupling (i.e., $r_{u,1} = r_{u,2} = r_{v,1} = r_{v,2} = 0$) satisfy Lemma 2.

Systems $\Sigma_{1,2}$ are now coupled by a diffusive connection,

$$\begin{aligned} r_{u,1} &:= \varepsilon(u_2 - u_1), \quad r_{v,1} := \varepsilon(v_2 - v_1), \\ r_{u,2} &:= \varepsilon(u_1 - u_2), \quad r_{v,2} := \varepsilon(v_1 - v_2), \end{aligned} \tag{13}$$

where $\varepsilon \geqslant 0$ denotes the coupling strength. This type of connection is a conventional coupling for two reaction-diffusion systems (see [26,27,33,34,40–43] for more details). Systems (12) with coupling (13) also have a spatially uniform steady state,

$$\begin{aligned} \boldsymbol{u}^* &:= [u_1\ v_1\ u_2\ v_2]^T \\ &= [u^*\ v^*\ u^*\ v^*]^T, \quad \forall x \in [0,L]. \end{aligned} \tag{14}$$

The local dynamics around steady state (14) are given by

$$\begin{aligned} \frac{\partial}{\partial t}\begin{bmatrix} \boldsymbol{\mathcal{X}}_1 \\ \boldsymbol{\mathcal{X}}_2 \end{bmatrix} &= \begin{bmatrix} \boldsymbol{A} - \varepsilon\boldsymbol{I}_2 & \varepsilon\boldsymbol{I}_2 \\ \varepsilon\boldsymbol{I}_2 & \boldsymbol{A} - \varepsilon\boldsymbol{I}_2 \end{bmatrix}\begin{bmatrix} \boldsymbol{\mathcal{X}}_1 \\ \boldsymbol{\mathcal{X}}_2 \end{bmatrix} \\ &\quad + \frac{\partial^2}{\partial x^2}\begin{bmatrix} \boldsymbol{D} & \boldsymbol{0} \\ \boldsymbol{0} & \mu\boldsymbol{D} \end{bmatrix}\begin{bmatrix} \boldsymbol{\mathcal{X}}_1 \\ \boldsymbol{\mathcal{X}}_2 \end{bmatrix}, \end{aligned} \tag{15}$$

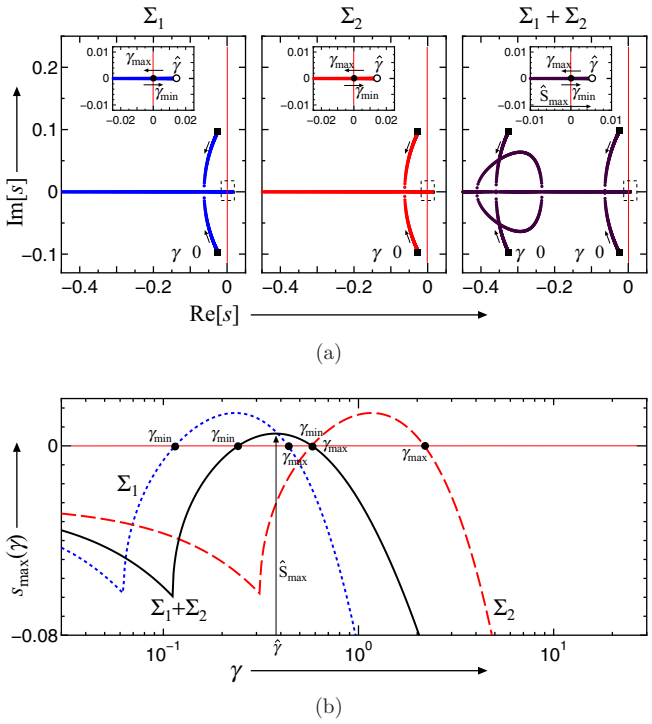


FIG. 1. Roots $s$ of the characteristic equations for system $\Sigma_1$ $[F(s,\gamma)=0]$, system $\Sigma_2$ $[F(s,\gamma\mu)=0]$, and coupled systems $\Sigma_1+\Sigma_2$ $[G(s,\gamma)=0]$, with $\varepsilon=0.15$ and $\mu=0.20$ as a function of $\gamma\geqslant 0$: (a) all of the roots $s_i(\gamma)$ $(i=1,\ldots,n)$ on the complex plane, and (b) real parts of the dominant roots $s_{\max}(\gamma)$.

where we have $\boldsymbol{\mathcal{X}}_{1,2}:=[u_{1,2}-u^* \quad v_{1,2}-v^*]^T$. The characteristic function of the linear system (15),

$$G(s,\gamma) := \det\left(s\boldsymbol{I}_4-\begin{bmatrix}\boldsymbol{A}-\varepsilon\boldsymbol{I}_2 & \varepsilon\boldsymbol{I}_2\\ \varepsilon\boldsymbol{I}_2 & \boldsymbol{A}-\varepsilon\boldsymbol{I}_2\end{bmatrix}+\gamma\begin{bmatrix}\boldsymbol{D} & \boldsymbol{0}\\ \boldsymbol{0} & \mu\boldsymbol{D}\end{bmatrix}\right), \tag{16}$$

allows us to obtain a sufficient condition for steady state (14) to be unstable.

*Lemma 3:* Systems $\Sigma_{1,2}$ under Assumption 1 are coupled by a diffusive connection (13). If systems $\Sigma_{1,2}$ are identical (i.e., $\mu=1$), there exists a length $L$ and boundaries such that the spatially uniform steady state (14) is unstable independently of $\varepsilon$.

*Proof.* For $\mu=1$, the characteristic function (16) is reduced to

$$G(s,\gamma)=F(s,\gamma)\det\left[s\boldsymbol{I}_2-\boldsymbol{A}+\gamma\boldsymbol{D}+2\varepsilon\boldsymbol{I}_2\right]. \tag{17}$$

Since there exists $\gamma\geqslant 0$ such that $F(s,\gamma)$ defined in Eq. (4) under Assumption 1 is unstable, there also exists $\gamma\geqslant 0$ such that $G(s,\gamma)$ with $\mu=1$ is unstable independently of $\varepsilon$. ■

A similar result to Lemma 3 for coupled *oscillators* has been reported in a previous study [44].

Here we provide the condition for steady state (14) to be stable.

*Theorem 1:* Systems $\Sigma_{1,2}$ under Assumption 1 are coupled by a diffusive connection (13). The spatially uniform steady state (14) is stable for any $L$ and boundary condition if and only if the characteristic function $G(s,\gamma)$ defined in Eq. (16) is stable for any $\gamma\geqslant 0$.

*Proof.* As this theorem is an obvious consequence of the above discussion, the proof is omitted. ■

We remark that it is easy to analyze the stability of $G(s,\gamma)$, since it can be described by a degree-four polynomial. The next section will show some numerical results with the well-known Brusselator model.

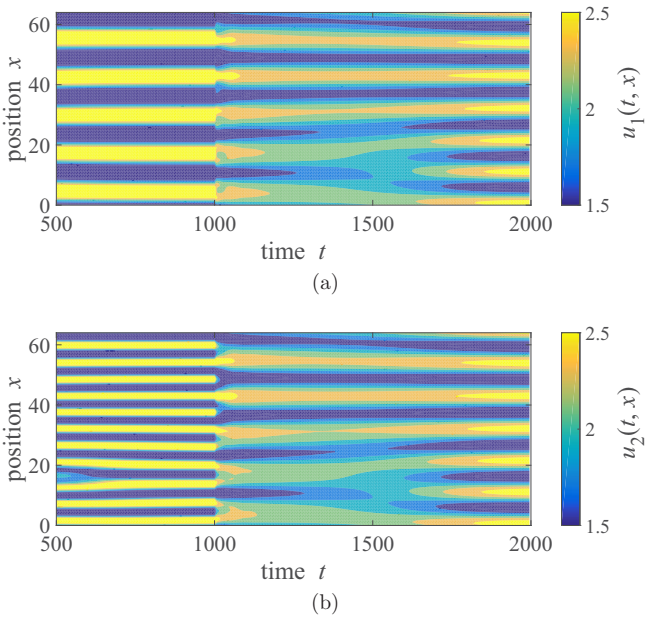


FIG. 2. Time series of $u_{1,2}$ before and after coupling with $\varepsilon=0.15$ and $\mu=0.20$: (a) $u_1(t,x)$ and (b) $u_2(t,x)$. Systems $\Sigma_{1,2}$ are coupled at $t=1000$.

## IV. NUMERICAL EXAMPLES

This section shows that the analytical results presented above are valid through numerical simulations. The present paper deals with the Brusselator model, a well-known reaction-diffusion system [21]. The reaction terms,

$$\begin{aligned} f(u,v)&=\eta\{a-(1+b)u+u^2v\},\\ g(u,v)&=\eta\{bu-u^2v\}, \end{aligned} \tag{18}$$

have an equilibrium point $(u^*,v^*)=(a,b/a)$, where $a>0$ and $b>0$ are the parameters. The parameter $\eta>0$ is used to transform the Brusselator model [21] into dimensionless form (1). The Jacobian matrix $\boldsymbol{A}$ around the equilibrium point has four elements: $f_u=\eta(b-1)$, $f_v=\eta a^2$, $g_u=-\eta b$, and $g_v=-\eta a^2$.

The parameters of the reaction terms (18) are set as

$$a=2.0,\quad b=4.0,\quad \eta=1/20.$$

These parameters satisfy inequalities (5) and (6) in Lemma 1 and inequality (9) in Corollary 1. The condition (10) in Lemma 2 is described by $\delta\in(0,1/4)$; thus, we set $\delta=0.2$. Both systems $\Sigma_{1,2}$ have length $L=64$ and a periodic boundary.

Here, the ratio of the diffusion coefficient for system $\Sigma_2$ and the coupling strength are set to $\mu=0.20$ and $\varepsilon=0.15$,

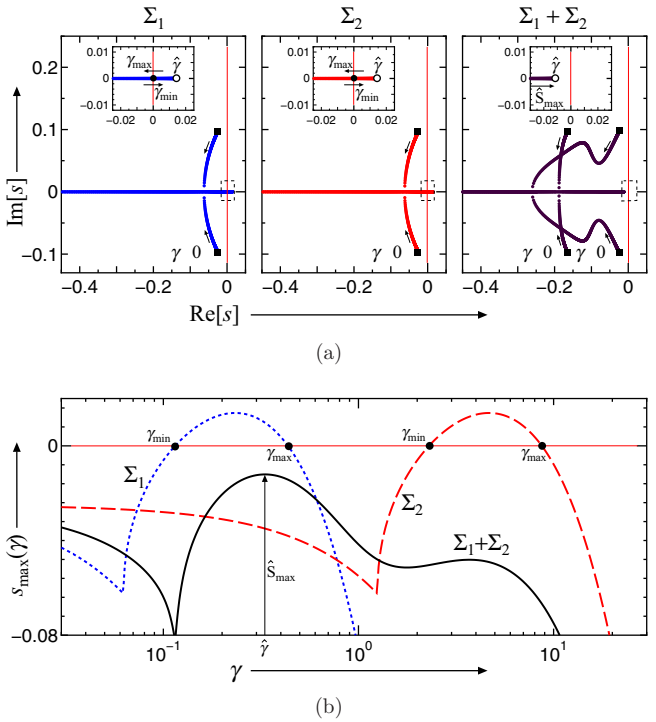


FIG. 3. Roots $s$ of the characteristic equations for system $\Sigma_1$ [$F(s,\gamma)=0$], system $\Sigma_2$ [$F(s,\gamma\mu)=0$], and coupled systems $\Sigma_1+\Sigma_2$ [$G(s,\gamma)=0$], with $\varepsilon=0.07$ and $\mu=0.05$ as a function of $\gamma\geqslant 0$: (a) all of the roots $s_i(\gamma)$ ($i=1,\ldots,n$) in the complex plane, and (b) real parts of the dominant roots $s_{\max}(\gamma)$.

respectively. The roots $s$ of the characteristic equations for the individual systems $\Sigma_1$ [i.e., $F(s,\gamma)=0$] and $\Sigma_2$ [i.e., $F(s,\gamma\mu)=0$], and coupled systems $\Sigma_1+\Sigma_2$ [i.e., $G(s,\gamma)=0$] as a function of $\gamma\geqslant 0$ are illustrated in Fig. 1(a). The real parts of the dominant roots for these equations,

$$s_{\max}(\gamma):=\max_{i\in\{1,\ldots,n\}}\mathrm{Re}[s_i(\gamma)], \tag{19}$$

with $n=2$ for $F(s,\gamma)=0$ and $F(s,\gamma\mu)=0$ and $n=4$ for $G(s,\gamma)=0$, against $\gamma$ are plotted in Fig. 1(b). For individual systems $\Sigma_1$ [i.e., $F(s,\gamma)=0$] and $\Sigma_2$ [i.e., $F(s,\gamma\mu)=0$], a pair of roots leave $\gamma=0$ (■), and one of them crosses the imaginary axis from left to right at $\gamma=\gamma_{\min}$ and crosses it again at $\gamma=\gamma_{\max}$ [see the insets in Fig. 1(a)]. This indicates that $F(s,\gamma)$ and $F(s,\gamma\mu)$ are unstable for $\gamma\in(\gamma_{\min},\gamma_{\max})$. For coupled systems $\Sigma_1+\Sigma_2$ [i.e., $G(s,\gamma)=0$], four roots leave $\gamma=0$ (■), and one of them crosses the imaginary axis from left to right at $\gamma=\gamma_{\min}$ and reaches the maximum positive value (◯),

$$\hat{s}_{\max}:=\max_{\gamma\geqslant 0}s_{\max}(\gamma) \tag{20}$$

at $\gamma=\hat{\gamma}$.

It follows from the behavior of the roots illustrated in Fig. 1 that Turing instability can occur in systems $\Sigma_{1,2}$ coupled by diffusive connection (13). The time series[3] of variables $u_{1,2}$ before and after coupling are shown in Fig. 2. Systems $\Sigma_1$ and $\Sigma_2$ behave independently, and respectively induce the Turing patterns with a low wave number and a high wave number until $t=1000$, when they are coupled by a diffusive connection (13). It can be seen that these Turing patterns merge into a single Turing pattern with a middle wavelength between those of the original patterns after coupling.

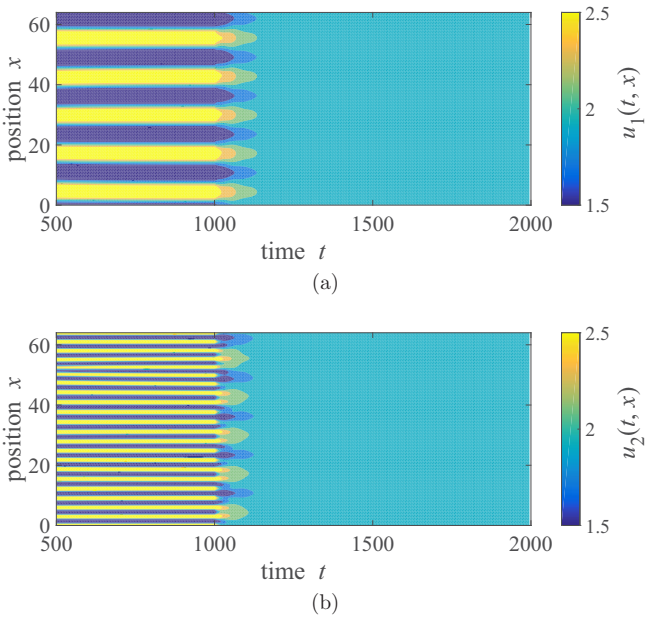


FIG. 4. Time series of $u_{1,2}$ before and after coupling with $\varepsilon=0.07$ and $\mu=0.05$: (a) $u_1(t,x)$ and (b) $u_2(t,x)$. Systems $\Sigma_{1,2}$ are coupled at $t=1000$.

Let us change the parameters to $\varepsilon=0.07$ and $\mu=0.05$. Figure 3 shows the roots $s$ for system $\Sigma_1$, system $\Sigma_2$, and coupled systems $\Sigma_1+\Sigma_2$. For systems $\Sigma_{1,2}$, a pair of roots leave $\gamma=0$ (■), and one of them crosses the imaginary axis from left to right and crosses again [see the insets in Fig. 3(a)]. For coupled systems $\Sigma_1+\Sigma_2$, four roots leave $\gamma=0$ (■); one of these roots reaches the maximum value (◯) but does not cross the imaginary axis: we have $\hat{s}_{\max}<0$.

From Fig. 3, we expect that Turing instability never occurs in systems $\Sigma_{1,2}$ coupled by connection (13). Figure 4 illustrates the time series of variables $u_{1,2}$ before ($t<1000$) and after ($t\geqslant 1000$) coupling. The Turing patterns after coupling disappear and a spatially uniform steady state (14) appears.

We numerically investigate the relation between the largest real part of the roots $\hat{s}_{\max}$ and the parameters $(\varepsilon,\mu)$. Here $\hat{s}_{\max}$ is plotted[4] in the parameter space $(\varepsilon,\mu)\in[0.0,0.2]\times[0.0,0.3]$, as illustrated in Fig. 5. The stable region with $\hat{s}_{\max}<0$ satisfies Theorem 1; thus, if $\varepsilon$ and $\mu$ are within this region, the spatially uniform steady state (14) becomes stable for any $L$ and any boundary condition. The parameter set $(\varepsilon,\mu)=(0.15,0.20)$ for the time series shown in Fig. 2 is outside of the stable region, but the parameter set $(\varepsilon,\mu)=(0.07,0.05)$ for Fig. 4 is inside of it. These time-series data agree with this stable region.

[3]The explicit Euler method (time step $10^{-4}$ and 512 space mesh points) is used for numerical integration.

[4]$\hat{s}_{\max}$ is estimated from the range $\gamma\in[0,10]$ for a $50\times 50$ grid in $(\varepsilon,\mu)$ space.

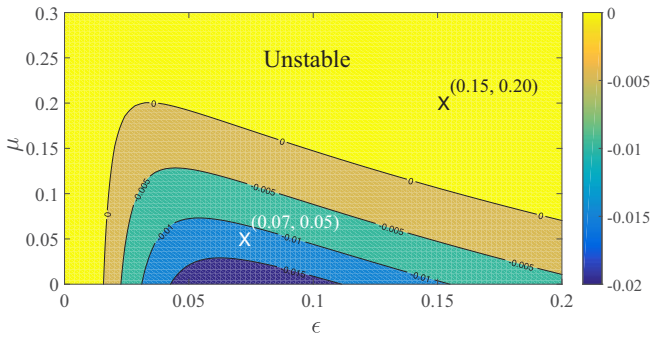


FIG. 5. Largest real part of the roots $\hat{s}_{\max}$ in parameter space $\varepsilon - \mu$. The yellow area denotes the unstable region and the other colors are the stable regions.

## V. DISCUSSION

This section reviews the previous studies related to our present paper in detail: phenomena in coupled reaction-diffusion systems with Turing patterns and those in stable oscillator networks. A large number of studies have been conducted on phenomena occurring in coupled reaction-diffusion systems with Turing patterns. A variety of phenomena induced by diffusive connections have been found, such as black eye and white eye patterns [33], symmetric, asymmetric, and antiphase patterns [34], and square patterns [35]. Diffusive connections have been experimentally implemented in real systems [36,37]. Furthermore, some types of couplings, such as dynamic connections [38], connections with distributed delays [39], and nonlinear connections [45], have been studied. It was reported that Turing patterns are induced in coupled reaction-diffusion systems whose reaction terms are different [43]. Ji and Li found that individual reaction-diffusion systems with a Turing pattern and with oscillatory behavior converge to a steady state after coupling [40]. We may say that this phenomenon corresponds to amplitude death in coupled reaction-diffusion systems. On the other hand, the present paper shows that amplitude death can occur even when both systems exhibit Turing patterns.

Recently, Turing patterns in oscillator networks have attracted great attention. Nakao and Mikhailov found that Turing instability occurs in large random networks whose nodes have stable dynamics [46]. This phenomenon was also observed in Cartesian product networks [47], where an extended version of Lemma 3 for Cartesian product networks was provided. Asllani *et al.* reported the following interesting result: for two Watts-Strogatz networks with different rewiring probabilities and diffusion constants, where one of the networks induces Turing instability and another does not, and they are coupled by a diffusive connection, a spatially uniform steady state can become stable [48]. This result is likely related to the stabilization considered in the present paper; however, the relation is not clear at present. Further insight into the relation is left for future work.

## VI. CONCLUSION

The present paper investigated the dynamics around a spatially uniform steady state in a coupled reaction-diffusion system with Turing instability. The main results obtained in this paper are summarized as follows: it was shown that stabilization does not occur in identical systems (see Lemma 3), and a condition for the steady state to be stable for any system length and types of boundaries was derived (see Theorem 1). Our main analytical results were supported with numerical simulations.

## ACKNOWLEDGMENT

The authors thank the anonymous reviewer for valuable comments and suggestions. This work was partially supported by JSPS KAKENHI Grant No. JP26289131.

## APPENDIX A: COMMENTS ON SYSTEM (1)

System (1) is similar to the dimensionless reaction diffusion system in Sec. 2.2 of [32]. The differences with system (1) are as follows: the coefficients of $\partial^2 u/\partial x^2$ and $\partial^2 v/\partial x^2$ are 1 and $d \in [1, +\infty)$, respectively. We remark that the range of the diffusion coefficient ratio in system (1) is finite for $\delta \in (0,1)$. The reason for our employing system (1) is the finite range for the ratio being more convenient for investigating stability in numerical simulations.

## APPENDIX B: PROOF OF LEMMA 2

This proof indicates that the diffusion coefficient ratio $\delta$, which satisfies both conditions (7) and (8) in Lemma 1 under assumption (9), can be described by Eq. (10). First, we consider condition (7). Under assumption (9), the ratio $\delta$ satisfying (7) can be described by

$$\delta \in (0, -f_u/g_v). \tag{B1}$$

Second, we deal with condition (8). As the left-hand side of inequality (8) is a quadratic downward-convex function of $\delta$, condition (8) holds for $\delta$ satisfying

$$\delta \in (0, \delta_-) \cup (\delta_+, +\infty), \tag{B2}$$

$$\delta_+ := \frac{f_u g_v - 2 f_v g_u + 2\sqrt{f_v g_u (f_v g_u - f_u g_v)}}{g_v^2}. \tag{B3}$$

Condition (6), and Eqs. (11) and (B3) suggest that $\delta_- < -f_u/g_v < \delta_+$ holds. Thus, $\delta$ satisfying both inequalities (B1) and (B2) is given by condition (10).

[1] G. Saxena, A. Prasad, and R. Ramaswamy, Phys. Rep. **521**, 205 (2012).
[2] A. Koseska, E. Volkov, and J. Kurths, Phys. Rep. **531**, 173 (2013).
[3] D. Aronson, G. Ermentrout, and N. Kopell, Physica D **41**, 403 (1990).
[4] R. Mirollo and S. Strogatz, J. Stat. Phys. **60**, 245 (1990).
[5] Y. Yamaguchi and H. Shimizu, Physica D **11**, 212 (1984).

[6] K. Bar-Eli, Physica D **14**, 242 (1985).
[7] A. Koseska, E. Volkov, and J. Kurths, Phys. Rev. Lett. **111**, 024103 (2013).
[8] Y. Wu, W. Liu, J. Xiao, W. Zou, and J. Kurths, Phys. Rev. E **85**, 056211 (2012).
[9] D. V. Ramana Reddy, A. Sen, and G. L. Johnston, Phys. Rev. Lett. **80**, 5109 (1998).
[10] D. Reddy, A. Sen, and G. Johnston, Physica D **129**, 15 (1999).
[11] F. Atay, Phys. Rev. Lett. **91**, 094101 (2003).
[12] M. Mehta and A. Sen, Phys. Lett. A **355**, 202 (2006).
[13] W. Zou, C. Yao, and M. Zhan, Phys. Rev. E **82**, 056203 (2010).
[14] Y. Sugitani, K. Konishi, L. B. Le, and N. Hara, Chaos **24**, 043105 (2014).
[15] W. Michiels and H. Nijmeijer, Chaos **19**, 033110 (2009).
[16] K. Konishi, Phys. Rev. E **68**, 067202 (2003).
[17] K. Konishi, Int. J. Bifurcations Chaos **17**, 2781 (2007).
[18] K. Konishi and N. Hara, Phys. Rev. E **83**, 036204 (2011).
[19] V. Resmi, G. Ambika, and R. E. Amritkar, Phys. Rev. E **84**, 046212 (2011).
[20] A. Sharma, P. R. Sharma, and M. D. Shrimali, Phys. Lett. A **376**, 1562 (2012).
[21] M. Cross and H. Greenside, *Pattern Formation and Dynamics in Nonequilibrium Systems* (Cambridge University Press, Cambridge, UK, 2009).
[22] R. C. Desai and R. Kapral, *Dynamics of Self-Organized and Self-Assembled Structures* (Cambridge University Press, Cambridge, UK, 2009).
[23] K. Ishimura, K. Komuro, A. Schmid, T. Asai, and M. Motomura, Nonlin. Theor. Appl., IEICE **6**, 252 (2015).
[24] D. Winston, M. Arora, J. Maselko, V. Gaspar, and K. Showalter, Nature (London) **351**, 132 (1991).
[25] J. Bragard, S. Boccaletti, and F. Arecchi, Int. J. Bifurcation Chaos **11**, 2715 (2001).
[26] S. Boccaletti, J. Bragard, F.T. Arecchi, and H. Mancini, Phys. Rev. Lett. **83**, 536 (1999).
[27] H. Nie, J. Gao, and M. Zhan, Phys. Rev. E **84**, 056204 (2011).
[28] I. S. Aranson and L. Kramer, Rev. Mod. Phys. **74**, 99 (2002).
[29] B. Shraiman, A. Pumir, W. van Saarloos, P. Hohenberg, H. Chate, and M. Holen, Physica D **57**, 241 (1992).
[30] H. Chate, Nonlinearity **7**, 185 (1994).
[31] H. Teki, K. Konishi, and N. Hara, Phys. Rev. E **95**, 062220 (2017).
[32] J. D. Murray, *Mathematical Biology II* (Springer-Verlag, New York, 2003).
[33] L. Yang, M. Dolnik, A. M. Zhabotinsky, and I. R. Epstein, Phys. Rev. Lett. **88**, 208303 (2002).
[34] L. Yang and I. R. Epstein, Phys. Rev. E **69**, 026211 (2004).
[35] J. Li, H. Wang, and Q. Ouyang, Chaos **24**, 023115 (2014).
[36] D. G. Miguez, M. Dolnik, I. Epstein, and A. P. Munuzuri, Phys. Rev. E **84**, 046210 (2011).
[37] L. Dong, Z. Shen, B. Li, and Z. Bai, Phys. Rev. E **87**, 042914 (2013).
[38] L. Yang and I. R. Epstein, Phys. Rev. Lett. **90**, 178303 (2003).
[39] L. Ji and Q. Li, J. Chem. Phys **123**, 094509 (2005).
[40] L. Ji and Q. Li, Chem. Phys. Lett. **424**, 432 (2006).
[41] J. Yang, Phys. Rev. E **76**, 016204 (2007).
[42] J. Gao, L. Xie, H. Nie, and M. Zhan, Chaos **20**, 043132 (2010).
[43] H. Fujita and M. Kawaguchi, J. Theor. Biol. **322**, 33 (2013).
[44] K. Konishi, Phys. Lett. A **341**, 401 (2005).
[45] K. Kytta, K. Kaski, and R. Barrio, Physica A **385**, 105 (2007).
[46] H. Nakao and A. S. Mikhailov, Nat. Phys. **6**, 544 (2010).
[47] M. Asllani, D. M. Busiello, T. Carletti, D. Fanelli, and G. Planchon, Sci. Rep. **5**, 12927 (2015).
[48] M. Asllani, D. M. Busiello, T. Carletti, D. Fanelli, and G. Planchon, Phys. Rev. E **90**, 042814 (2014).